Journal of Integrative Neuroscience, Vol. 15, No. 4 (2016) 571–591

DOI: 10.1142/S021963521650031X

World Scientific
www.worldscientific.com

Conflicting effects by antibodies against connexin36 during the action of intracellular Cyclic-AMP onto electrical synapses of retinal ganglion cells

Soh Hidaka*

Department of Physiology
Fujita Health University School of Medicine
Toyoake Aichi 470-1192, Japan
**shidaka@fujita-hu.ac.jp*

[Received 18 August 2016; Accepted 7 November 2016; Published 5 January 2017]

Alpha-type retinal ganglion cells (alpha cells) of the same class in mammalian retina are connected by gap junctions. Electrical synapses between alpha cells were examined using combined techniques of dual patch-clamp recordings, intracellular labeling and electron microscopy in the albino rat retina. In simultaneous dual whole-cell recordings from pairs of neighboring alpha cells, bidirectional electrical synapses with symmetrical junction conductance were observed in pairs with cells of the same morphological type. Regulatory domains of gap junction protein subunit connexins in electrical synapses between alpha cells by extracellular and intracellular ligands investigated by dual whole-patch clamp recordings. I examined how passage currents through electrical synapses between alpha cells are modulated by specific antibodies against connexin36 proteins, and extracellular or intracellular application of ligands. Control conditions led us to observe large passage currents between connected cells and adequate transjunctional conductance (Gj) (1.35 ± 0.51 nS). Experimental results show that high level of intracellular cyclic AMP within examined cells suppress electrical synapses between the neighboring cells. Gj between examined cells reduced to 0.15 ± 0.04 nS. Under application of dopamine (1.25 ± 0.06 nS) or intracellular cyclic GMP (0.98 ± 0.23 nS), however, Gj also remains as in the control level. Intracellular application of an antibody against the cytoplasmic loop of connexin36 reduced G_j (0.98 ± 0.23 nS). Cocktail of the antibody against cytoplasmic connexin36 and intracellular cyclic AMP leaves Gj as in the level by single involvement of the cytoplasmic antibody. The elimination of Gj by the cytoplasmic antibody was in a dose-dependent manner. These results suggest that binding domains against cyclic AMP may be present in the cytoplasmic sites of connexin proteins to regulate channel opening of gap junctions between mammalian retinal alpha ganglion cells.

Keywords: Retinal ganglion cells; gap junction; connexin; electrical synapse; cyclic AMP; cytoplasmic antibody; high voltage electron microscopy.

Nomenclature

ABC	Avidin-biotin-HRP complex
cAMP	Adenosine 3′, 5′-cyclic monophosphate

cGMP	Guanosine 3′, 5′-cyclic monophosphate
Cx	Connexin
DAB	Diaminobenzidine
Gj	Electrical junction conductance
GCL	Ganglion cell layer
HRP	Horseradish peroxidase
INL	Inner nuclear layer
IP_3,	Inositol 1,4,5-trisphosphate
IPL	Inner plexiform layer
LY	Lucifer Yellow
OPL	Outer plexiform layer
PBS	Phosphate buffer saline
s-a	Sublamina-a of the IPL
s-b	Sublamina-b of the IPL
TBS	Tris-buffered saline

1. Introduction

Gap junctions are intercellular membrane channels that subserve direct cell-to-cell communication for the exchange of ions and small molecules resulting in metabolic and electrical coupling of cells (Bennett *et al.*, 1991). Individual intercellular channels are dodecameric structures consisting of two hexameric connexons (channel protein particles), provided by either of the two communicating cells. Gap junctions are made up of clusters that are aggregates of connexons. Each connexon is a hexameric structure composed of subunit proteins called connexins, each of which has four transmembrane domains. The connexins represent a family of proteins composed of a variety of members known to exist in mammalian tissue (Bruzzone *et al.*, 1996; Goodenough *et al.*, 1996; White & Paul, 1999).

In the vertebrate retina, electrophysiological measurements and microinjection of tracer molecules have revealed extensive gap-junctional communication among every class of adult neurons (Naka & Christensen, 1981; Vaney, 1991, 1994; Hidaka, 2012; Hidaka *et al.*, 1993, 2004, 2005; Söhl *et al.*, 2005; Bloomfield & Völgyi, 2009; Völgyi *et al.*, 2013) and during neuronal development (Penn *et al.*, 1994). The transmission of electrical signals via gap-junctional pathways influences the response properties and receptive-field organization of adult retinal neurons (Mastronarde, 1983, 1989; Hidaka *et al.*, 1993, 2004, 2005; Umino *et al.*, 1994; Meister *et al.*, 1995; Poznanski & Umino, 1997; Bloomfield & Völgyi, 2004). Although many factors modulate gap-junctional communication in brain and retinal neurons, little is known about the molecular structure of the connexin proteins mediating these effects. Recently, I demonstrated that the permeability of gap junctions and the electrical synapses between retinal amacrine cells of goldfish were suppressed by intracellular application

February 6, 2017 6:17:04pm WSPC/179-JIN 1650031 ISSN: 0219-6352 2nd Reading

of high level of cyclic AMP (cAMP) (Hidaka, 2012). Dopamine or even high elevation of intracellular cyclic GMP (cGMP), however, left gap junction channels of these cells permeable to Neurobiotin into neighboring cells as in the control level. Electrical synapses between goldfish amacrine cells remained open under application of dopamine or intracellular cGMP. These results show that intracellular cAMP uncoupled certain types of amacrine cells. When intracellular cAMP is raised tonically in certain conditions, the findings demonstrate that intracellular cAMP uncouples the retinal circuit associated with the amacrine cells in the inner retina. A circuit switching system by suppression of electrical synapses between amacrine cells would be compatible with cAMP's other possible diverse functions, all of which is associated with the transition from scotopic to photopic vision. These results suggest that intracellular cAMP may directly act on cytoplasmic sites of gap junction connexin proteins. To support this idea, I will show whether intracellular cAMP associates gap junction connexins in this study.

Specific antibodies against gap junction connexin proteins can identify the presence and localization of gap junctions and electrical synapses between electrically coupled cells. Antibodies against cytoplasmic domains of connexins are also expected to modulate gap junction conductance of electrical synapses between connected cells by associating with connexin proteins. It was reported that other antibodies against cytoplasmic domains of inositol 1,4,5-trisphosphate (IP_3) receptors inhibited Ca^{2+} wave and Ca^{2+} oscillation through calcium channels Miyazaki *et al.* (1992) distinguished Ca^{2+} responses by IP_3-induced Ca^{2+} release from Ca^{2+}-induced Ca^{2+} release.

In the present study, I investigated whether electrical synapses between retinal neurons modulated by intracellular application of cyclic AMP and antibodies against connexins. Antibodies against cytoplasmic loop of connexin36 (Hidaka *et al.*, 2002, 2004) mimicked the effects of intracellular cyclic AMP onto electrical synapses between alpha retinal ganglion cells.

2. Results

2.1. *Effects of electrical synapses between retinal ganglion cells by intracellular cyclic nucleotides*

Cell bodies of alpha retinal ganglion cells were identified by the size (more than 20 μm in diameter) and their characteristic nuclei (Tauchi *et al.*, 1992) under Nomarski differential interference illumination. I targeted closely located large cell bodies of more than 20 μm in diameter, and examined two larger cell bodies of about 100–200 μm apart [Fig. 1(a)], because they could probably be selected for retinal ganglion cells (alpha cells) of the same morphological type (Peichl, 1989; Peichl *et al.*, 1987; Tauchi *et al.*, 1992). Rat alpha-type retinal ganglion cells were coupled with each other when Neurobiotin was intracellularly injected into the cell via a micropipette. Alpha cells of the same morphological type were distributed in a regular

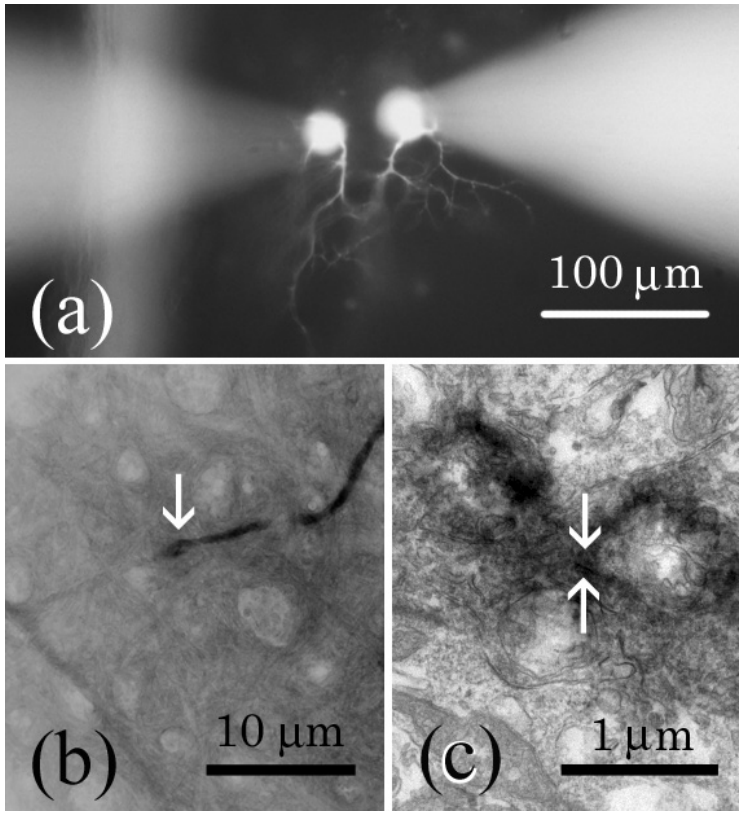

Fig. 1. Rat alpha retinal ganglion cells for dual whole-cell patch-clamp recordings and electron micrographs showing dendrodendritic contacts between electrically coupled neighboring cells. (a), Fluorescence photomicrograph of a pair of alpha retinal ganglion cells in a whole-mount preparation after filling with LY for dual whole-cell patch-clamp recordings. Scale bar: 100 μm. (b), A junctional contact (arrow) occurs between the tips of peripheral dendrites from Neurobiotin-coupled alpha cells by high voltage electron microscopy. The specimen was observed at 1000 kV in a tangential 5 μm section in thickness. (c), Immunocytochemical labeling of junctional contacts between alpha cells by anti- connexin36 antibody. A gap junction (***arrows***) formed between two labeled peripheral dendrites by conventional electron microscopy of an ultrathin section at 75 kV. The antibody labeled the cytoplasmic sites of gap junctions at two apposed membranes between the contacted alpha cells. Scale bars: 10 μm for (b), and 1 μm for (c).

hexagonal array (Hidaka *et al.*, 2004). Figure 1(b) shows dendrodendritic contacts (arrowheads) occurred between the labeled cells by high-voltage electron microscopy of thick sections in production of a three-dimensional view of the contacts (Hidaka *et al.*, 1986, 1993). Figure 1(c) shows immunocytochemical labeling of alpha cells by anti- connexin36 (Cx36) antibody against cytoplasmic loop of Cx36 protein (Hidaka *et al.*, 2002, 2004). Anti-Cx36 antibody labeled junctional contacts between the rat alpha cells [arrowheads in Fig. 1(c)]. Ultrastructural analysis revealed that the antibody labeled the cytoplasmic sites of gap junctions at two apposed membranes between the contacted cells [Fig. 1(c)]. These results confirmed the presence of gap

junctions consisting of connexin36 between alpha cells, in the previous results as reported by Hidaka *et al.* (2002, 2004).

Dual whole-cell patch-clamp recordings in control condition measure electrical junction conductance (Gj) in pairs of alpha cells [Fig. 1(a)]. The junction conductance was estimated with both cells in voltage clamp by applying a series of test voltages to the presynaptic cell and recording the generated currents in both the pre- and the postsynaptic cell (Fig. 2). The relationship between junction voltage (Vj) and junction current (Ij) was linear [Fig. 2(b)], when corrected for nonzero series resistance and finite membrane input resistance. This result indicates that **Gj** was independent of Vj over the range of test voltages (±30 mV). The junctional conductance was then measured as the slope of a straight line fitted to the I–V relation [1.72 nS, Fig. 2(b)]. The Gj for a cell pair was calculated as the slope conductance determined from each direction of coupling and plotted for both directions of coupling for each cell pair [Fig. 2(b)]. This result shows that the electrical junction conductance of alpha cells in control condition was symmetric without rectification

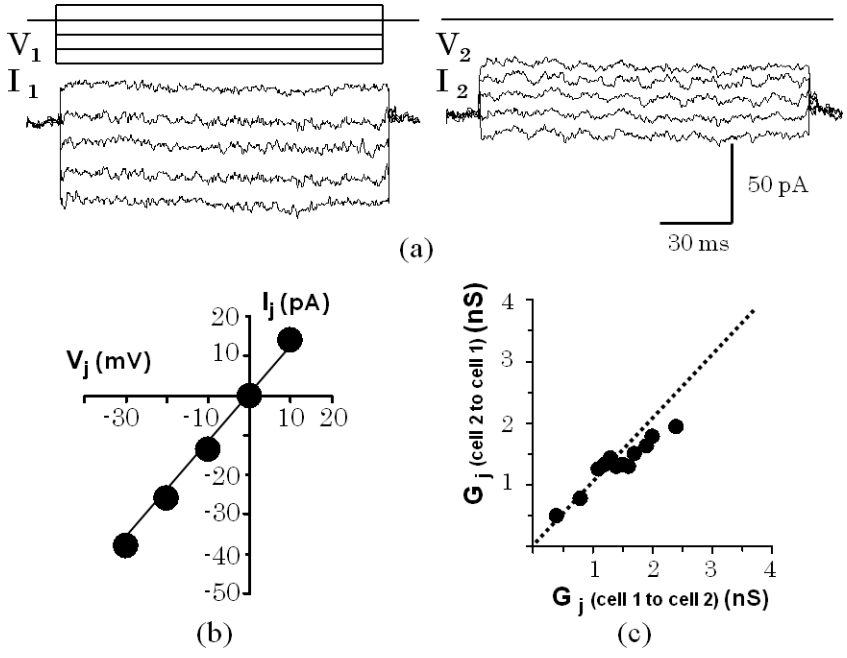

Fig. 2. Measurement of electrical junction conductance (Gj) between alpha cells. (a), With both cells in whole-cell voltage clamp (V1 and V2), voltage steps (−90 to −50 mV, 10 mV increments) from holding potential of −60 mV were applied to one cell (V1) and current responses were recorded in both cells (I1 and I2). (b), Current-voltage relationship between the junctional current (Ij) and the junctional voltage (Vj) shown in (a). The plotted data are fit with a straight line in which the slope shows Gj (1.72 nS). (c), Summary of Gj. Comparison of Gj in each direction shows nonrectifying electrical synapses, when electrical coupling in the same cell pair was examined in both directions [e.g., Gj (cell 1 to cell 2) for cell 1 presynaptic, and Gj (cell 2 to cell 1) for cell 2 presynaptic]. The dashed line indicates the values expected when Gj is the same in both directions for pairs of rat alpha cells.

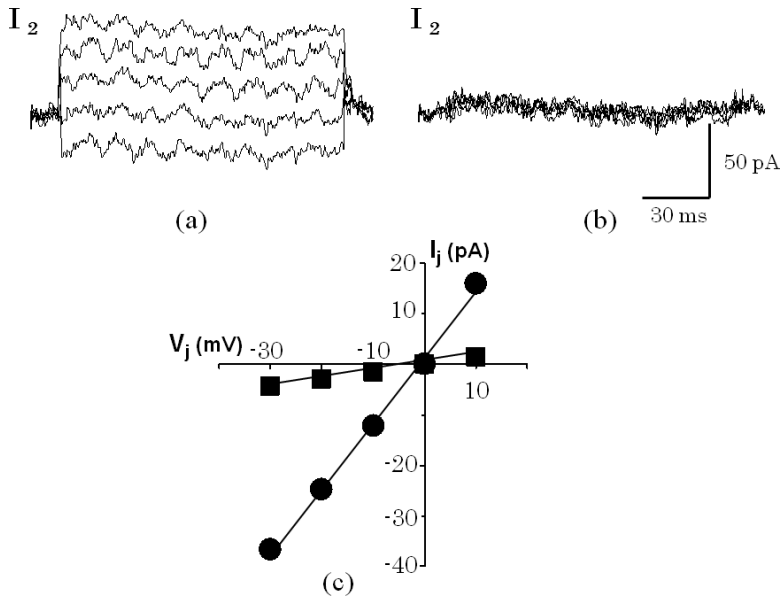

Fig. 3. Suppression of electrical synapses between alpha cells by intracellular cyclic AMP. High dose of intracellular cyclic AMP reduces electrical junction conductance (Gj) of rat alpha cells. (a), In a control condition, junctional currents (I_2) appeared in one cell when voltage steps (-90 to -50 mV, 10 mV increments) from holding potential of -60 mV with both cells in whole-cell voltage clamp were applied to the other cell. Average electrical junction conductance (Gj) between alpha cells for the control condition was 1.35 ± 0.51 nS ($n = 12$ pairs). (b), Involvement of 5 mM cyclic AMP in pipette decreased junctional currents (I_2) between alpha cells. (c), Comparison of current–voltage relationship between the junctional current and the junctional voltage shown for the control condition and involvement of cyclic AMP. From the plotted data for the control condition (circles) and involvement of cyclic AMP (squares), individual Gj were calculated by the slopes for straight lines fit with the data, 1.31 nS for the control condition and 0.15 nS for involvement of cyclic AMP, respectively.

[Fig. 2(c)]. The mean Gj for rat alpha cells was 1.35 ± 0.51 nS ($n = 12$ cell pairs; range 0.40–2.45 nS).

When patch pipettes with 5 mM cAMP were applied to a pair of alpha cells in dual whole-cell recordings, junction currents (I_2) were dramatically decreased [Fig. 3(b)]. Gj decreased to 0.15 ± 0.04 nS ($n = 4$ cell pairs), in the presence of intracellular cAMP [Fig. 3(c)]. These results demonstrate that a high dose of intracellular cAMP in alpha cells can block electrical synapses between them. Under application of 100 μM dopamine (1.16 ± 0.21 nS) or intracellular cyclic GMP (0.94 ± 0.22 nS), however, Gj also remains as in the control level.

2.2. *Effects of electrical synapses between alpha cells by intracellular application of specific antibodies against connexins*

Specific antibodies against connexin36 are expected to affect gap junction conductance by binding to cytoplasmic domains of gap junction proteins. To examine channel opening of electrical synapses by intracellular modulation, I applied anti-Cx36 antibody to cytoplasm of alpha cells. When patch pipettes with 5 μg/mL of

antibodies against cytoplasmic domains of connexin36 (Hidaka *et al.*, 2002, 2004) were applied to a pair of alpha cells in dual whole-cell recordings, junction currents (I_2) were decreased (Fig. 5). Gj decreased to 0.98 nS ± 0.23 nS ($n = 4$ cell pairs) in the presence of the antibodies [1.07 nS in Fig. 5(c)].

To investigate regulation of electrical synapses by intracellular cyclic AMP, I applied mixture of cyclic AMP and anti-Cx36 antibody to cytoplasm of rat alpha cells. When patch pipettes with cocktail of 5 mM cAMP and 5 μg/mL of anti-Cx36 antibody were applied to pair of alpha cells in dual whole-cell recordings, junction currents (I_2) were decreased [Fig. 4(b)]. Gj decreased to 0.90 nS ± 0.21 nS ($n = 4$ cell pairs) in the presence of mixture of cyclic AMP and anti-Cx36 antibody [Gj =

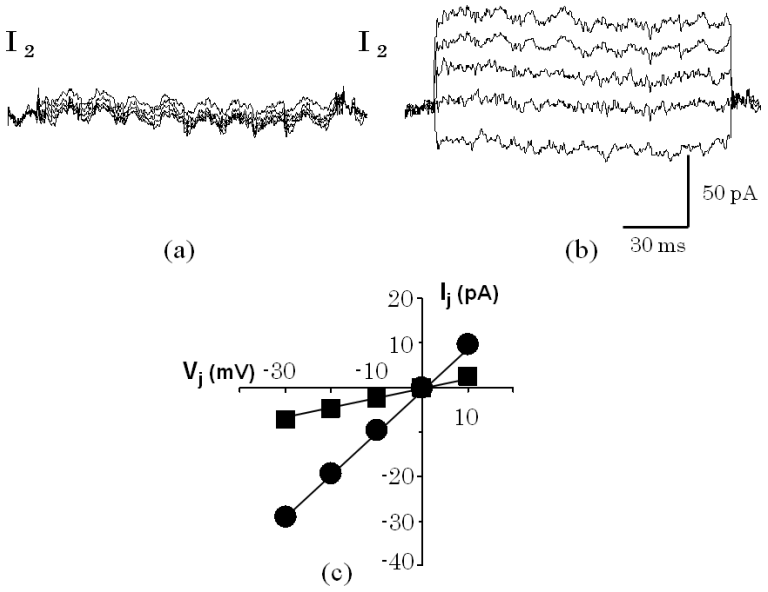

Fig. 4. Intracellular anti-Cx36 antibody competes with the suppression of electrical synapses between alpha retinal ganglion cells by intracellular cyclic AMP. (a), Involvement of mixture of 5 mM cyclic AMP and anti-Cx36 antibody with concentration of 0.1 μg/mL in pipette decreased junctional currents (I_2) between rat alpha cells. The antibody was raised against the cytoplasmic sites of gap junctions of Cx36. Intracellular cyclic AMP reduced Gj between alpha cells even with the presence of low concentration of anti-Cx36 antibody (0.1 μg/mL). (b), Junctional currents (I_2) between alpha cells by involvement of both 5 mM cyclic AMP and 5 μg/mL of anti-Cx36 antibody in pipette. The large junctional currents (I_2) remain even under intracellular cyclic AMP (5 mM) with the presence of concentration of anti-Cx36 antibody (5 μg/mL). (c) Comparison of current–voltage relationship between the junctional current and the junctional voltage shown for involvement of mixture of intracellular cyclic AMP and different concentrations of anti-Cx36 antibody. For concentration of anti-Cx36 antibody colocalized with 5 mM cyclic AMP in pipette, plots with low concentration of 0.1 μg/mL (squares) and high concentration of 5 μg/mL (circles) are shown, respectively. From the plotted data for the involvement of mixture of cyclic AMP with low concentration (0.1 μg/mL) of anti-Cx36 antibody (squares), and cyclic AMP and high concentration of (5 μg/mL) anti-Cx36 antibody (circles), individual Gj were calculated by the slopes for straight lines fit with the data, 0.23 nS for the involvement of low concentration of anti-Cx36 antibody, and 0.97 nS for high concentration of anti-Cx36 antibody, colocalized with cyclic AMP, respectively. The current–voltage relationship shows dose-dependency of anti-Cx36 antibody on effects of intracellular cyclic AMP.

1.08 nS, Fig. 4(c)]. In the presence of the anti-Cx36 antibody, the decrease of Gj, however, was quite small [Fig. 4(b)], compared with the application of intracellular cyclic AMP alone [Fig. 3(b)]. When patch pipette involved cocktail of cyclic AMP and anti-Cx36 antibody [Fig. 4(b)], however, Gj remained in the level of single involvement of the antibody [Fig. 5(a)]. The anti-Cx36 antibody blocked the effects of intracellular cyclic AMP. These results demonstrate that intracellular anti-Cx36 antibody suppressed the effect of intracellular cyclic AMP.

Next, I examined dose-dependency of anti-Cx36 antibody on effects of intracellular cyclic AMP. When patch pipette involved 0.1 μg/mL of anti-Cx36 antibody with 5 mM cyclic AMP, large suppression of Gj remained at 0.23 nS [Fig. 4(a)]. When small mount of the antibody with cyclic AMP was applied, the junctional currents through electrical synapses between alpha retinal ganglion cells were small, as seen in that of single application of cyclic AMP (5 mM). When 10-times higher concentration, 1 μg/ml of anti-Cx36 antibody with 5 mM cyclic AMP was applied, Gj increased to 0.73 nS (data not shown), but Gj was smaller compared with application of

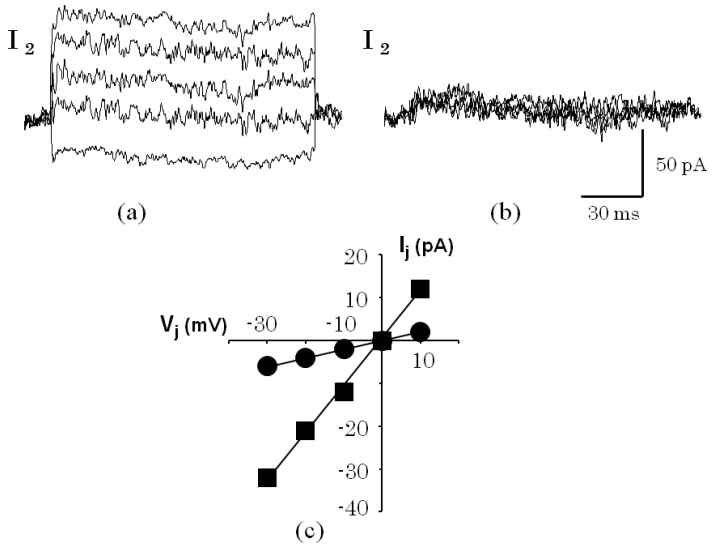

Fig. 5. Intracellular negative-control antibody, anti-Cx43 antibody, does not suppress the effects by intracellular cyclic AMP on electrical synapses between alpha retinal ganglion cells. (a), Involvement of anti-Cx36 antibody with concentration of 5 μg/mL in pipette generated junctional currents (I_2) between rat alpha cells. (b), Junctional currents (I_2) between alpha cells by involvement of both 5 mM cyclic AMP and 5 μg/mL of anti-Cx43 antibody in pipette. Intracellular cyclic AMP reduced Gj between alpha cells even with the presence of high concentration of anti-Cx43 antibody (5 μg/mL). Intracellular anti-Cx43 antibody does not compete with the suppression of electrical synapses between alpha cells by intracellular cyclic AMP. (c), Comparison of current–voltage relationship between the junctional current and the junctional voltage shown for involvement of intracellular anti-Cx36 antibody (5 μg/mL) and mixture of cyclic AMP and anti-Cx43 antibody (5 μg/mL). From the plotted data for the single involvement of anti-Cx36 antibody (squares) and mixture of cyclic AMP and anti-Cx43 antibody (circles) and, individual Gj were calculated by the slopes for straight lines fitting with the data, 1.07 nS for the single involvement of anti-Cx36 antibody and 0.20 nS for mixture of cyclic AMP and anti-Cx43 antibody, respectively.

5 μg/mL anti-Cx36 antibody [Fig. 4(b)]. These results show that binding of the antibody to cytoplasmic site of gap junctions competes with the effects of intracellular cyclic AMP. This study suggests that intracellular cyclic AMP affects the cytoplasmic domains of gap junctions of cells expressing connexin36, while cyclic AMP would fail to act on gap junctions with binding of anti-Cx36 antibody on their cytoplasmic domains.

To address this possibility that binding of anti-connexin36 antibody to cytoplasmic site of gap junctions competes with the effects of intracellular cyclic AMP, I examined intracellular application of other kind of negative-control antibody under the presence of high concentration of intracellular cyclic AMP. I applied anti-connexin43 (Cx43) antibody intracellularly. Connexin43 is a well-known connexin protein expressing gap junctions between astrocyte glia, and between retinal pigment epitheria (Janssen-Bienhold *et al.*, 1998; Dermietzel *et al.*, 2000). When patch pipette involved 5 μg/mL of anti-Cx43 antibody with 5 mM cyclic AMP, large suppression of Gj remained at 0.20 nS [Fig. 5(b)]. The decrease of junctional currents through electrical synapses between alpha cells was compatible to that of single application of 5 mM cyclic AMP [Fig 3(b)]. Even higher concentration of anti-Cx43 antibody (5 μg/mL) did not suppress the effect of intracellular cyclic AMP.

Electrical junction conductance of rat alpha retinal ganglion cells against applied ligands is summarized in Fig. 6. These results demonstrate that a high dose of intracellular cyclic AMP (5 mM) in alpha retinal ganglion cells can block electrical

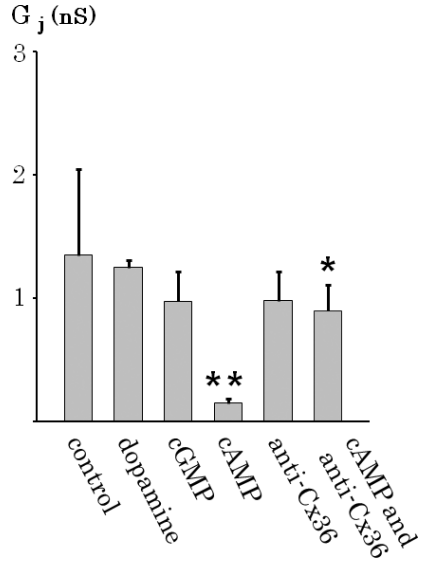

Fig. 6. Summary of electrical junction conductance (Gj) between alpha retinal ganglion cells when examined ligands were applied. Comparison of Gj under control conditions and applied ligands: dopamine (100 μM), cyclic GMP (cGMP, 5 mM), cyclic AMP (cAMP, 5 mM), anti-connexin36 antibody (anti-Cx36, 5 μg), and cocktail of cAMP (5 mM) and anti-Cx36 (5 μg, cAMP and anti-Cx36). Data are shown as mean $\pm$ SEM. Statistical significance was evaluated by Student's t-test. Gj under application of cocktail of cAMP and anti-Cx36 shows $^*p < 0.02$ to that of control conditions. Under application of cyclic AMP, $^{**}p < 0.002$ was demonstrated, compared with control condition.

synapses between them to the statistically dominated level (double asterisks in Fig. 6). Small elevation of intracellular cyclic AMP concentration within alpha cells by application of dopamine (100 μM), however, does not decrease electrical coupling between them. Even high elevation of intracellular cyclic GMP concentration (5 mM) does not appear to affect electrical coupling between them. Application of anti-Cx36 antibody (5 μg/mL) to cytoplasm of alpha cells decreases electrical coupling between them. Intracellular application of mixture of 5 mM cyclic AMP with 5 μg/mL of anti-Cx36 antibody leave large electrical coupling between alpha cells, although Gj decreased to the statistically dominated level (single asterisk in Fig. 6).

3. Discussion

The present study has measured modulation of electrical junctional conductance of gap junctions between rat alpha cells. This refines our knowledge about electrical synapses between cells. Although knowledge of regulation of gap junctions between mammalian alpha cells has been determined in several different ways (Hampson *et al.*, 1992; Kothmann *et al.*, 2009), this is the first report based on simultaneous measurement of regulation of electrical synapses between alpha cells by dual whole-cell patch clamp recordings. This approach has served to clarify effects of intracellular cAMP on gap junctions, and a more quantitative assessment about almost complete suppression of electrical synapses by high level of intracellular cAMP.

Significant uncoupling between alpha cells occurred by increased levels of cAMP. For measurement of electrical synapses by dual whole-cell patch clamp methods, several minutes after patching cells of a pair allowed permitting the cell cytosol to equilibrate with the pipette solution. When 5 mM cAMP was added in patch pipettes, significant amount of intracellular cAMP, introduced by patch pipettes, would diffuse to cytoplasm of alpha cells if the cAMP is in part degraded by possible phosphodiesterases in several minutes. Highly increased levels of intracellular cAMP need to suppress the junctional current of alpha cells. It is possible that cAMP would be directly associated with gap junctions of alpha cells. When anti-Cx36 antibody was added in patch pipettes, intracellular anti-Cx36 antibody induced significant uncoupling between alpha cells. Suppression of the junctional current of alpha cells by intracellular anti-Cx36 antibody was small, compared with the presence of cyclic AMP.

When mixture of cyclic AMP and anti-Cx36 antibody to cytoplasm of rat alpha cells was applied, Gj decreased in the presence of anti-Cx36 antibody with cyclic AMP. In the presence of the anti-Cx36 antibody, however, the decrease of Gj by intracellular cyclic AMP was quite small. Thus, introduction of intracellular anti-Cx36 antibody competes with the effect of intracellular cyclic AMP. I conclude that suppression of electrical synapses between these cells with dual patch clamp measurement is physiologically significant due to the occurrence by increased levels of

intracellular cAMP. Intracellular anti-Cx36 antibody can suppress the effect of intracellular cyclic AMP.

This study showed that high dose of intracellular cAMP can affect opening of gap junction channels between mammalian alpha cells. The experimental results by cocktail of cyclic AMP and the antibody suggest that cAMP would be directly associated with cytoplasmic subunits of gap junctions of mammalian alpha cells. Study by Miyazaki *et al.* (1992) showed cytoplasmic antibody against inositol 1,4,5-trisphosphate (IP_3) receptors blocked Ca^{2+} wave and Ca^{2+} oscillation generated in fertilized mammalian eggs. The antibody against IP_3 receptors distinguished Ca^{2+} wave and Ca^{2+} oscillation induced by Ca^{2+}-induced Ca^{2+} release from sperm-induced Ca^{2+} wave and Ca^{2+} oscillation by blocking IP_3-induced Ca^{2+} release. Their experiments by using the cytoplasmic antibody revealed that Ca^{2+} release in fertilized hamster eggs is mediated solely by the IP_3 receptor. Thus, cytoplasmic antibodies against ion channels or receptor proteins will bind to functional subunits of these physiological membrane proteins. Association with cytoplasmic subunits by the antibodies can induce to change physiological channel kinetics of gap junctions.

It is unknown neuromodulators, inducing highly rise of intracellular cAMP production that block gap junction channels of retinal ganglion cells. It is not possible that conventional physiological conditions induce highly raise of intracellular cAMP level to block of electrical coupling between the retinal ganglion cells. The present study has shown that intracellular cAMP uncouples the alpha cells. If we accept that intracellular cAMP is raised tonically in certain conditions, then the findings from the present study suggest that intracellular cAMP may uncouple the retinal circuit associated with the retinal ganglion cells in the inner retina.

The functional role of electrical synapses between alpha cells appears to be significant for scotopic vision. In the dark-adapted retina, the activity of receptive-field surrounding alpha cells is lost and the size of the receptive-field centers significantly increases (Barlow *et al.*, 1957; Peichl & Wässle, 1983; Muller & Dacheux, 1997). It is interesting how electrical synapses between alpha cells contribute to visual tasks under scotopic conditions. The contrast sensitivity of a neuron that integrates signals from photoreceptors in its field depends on the area of the receptive field; therefore large receptive fields would permit higher contrast sensitivity by improving the signal-to-noise ratio. Modeling studies of bipolar cells (Umino *et al.*, 1994; Poznanski & Umino, 1997) concluded that electrical coupling could smooth a signal over coupled cells, reducing the difference between central and peripheral cells by up to 80% before visual acuity was compromised. Therefore, low level of electrical coupling between alpha cells under mesopic conditions can contribute to noise reduction without comprising visual acuity. Under mesopic conditions, the sustained depolarizing responses of bipolar cells are barely apparent in sustained spikes of retinal ganglion cells, whereas under scotopic conditions, the transient spikes of the alpha cells is reflected in the light-evoked response of mammalian rod bipolar cells (Nelson, 1982; Kolb & Nelsen, 1983; Dacheux & Raviola, 1986). Such circuit switching would be

February 6, 2017 6:17:07pm WSPC/179-JIN 1650031 ISSN: 0219-6352 2nd Reading

compatible with cAMP's other possible diverse functions, all of which is associated with the transition from scotopic to photopic vision.

4. Conclusion

The purpose of this study was to elucidate regulation mechanisms of gap junctions and electrical synapses between mammalian retinal ganglion cells by internal messengers. The present study has measured gap junction conductance between mammalian alpha-type retinal ganglion cells. This approach has served to clarify effects of intracellular cAMP on gap junctions, including a quantitative assessment about almost complete suppression of electrical synapses by high level of intracellular cAMP. Intracellular anti-Cx36 antibody competes with the effect of intracellular cyclic AMP. High dose of intracellular cAMP affects opening of gap junction channels between mammalian alpha cells. The experimental results by cocktail of cyclic AMP and the antibody suggest that cAMP would be directly associated with gap junctions of mammalian alpha cells.

Highlight

To elucidate regulation mechanisms of gap junctions and electrical synapses between mammalian retinal ganglion cells by internal messengers, the present study has measured gap junction conductance between mammalian alpha cells.

The present study has clarified effects of intracellular cAMP on gap junctions including almost complete suppression of electrical synapses by high level of intracellular cAMP.

Intracellular anti-Cx36 antibody suppresses the effect of intracellular cyclic AMP.

The experimental results by cocktail of cyclic AMP and the antibody suggests that cAMP would be directly associated with gap junctions of mammalian alpha cells.

5. Experimental Procedure

5.1. *Animal use*

Experiments were carried out with 36 Wistar female rats (4 weeks to 4 months postnatal) weighing 50–250 g. Animal use was in accordance with the legislation by the Physiological Society of Japan regulating the use of animals in research, and the recommendations of the NIH Guide for the Care and Use of Laboratory Animals (National Institutes of Health, USA). Experiments by using animals are permitted by a committee for animal experiments within our university (permission number of this study; M 18-06). Animals were commercially supplied from a breeder (Japan SLC, Inc., Hamamatsu. Shizuoka, Japan), and maintained with the light phase from 7:00 a.m. to 7:00 p.m. in an animal room under control of temperature at 23°C until use. The animals were deeply anaesthetized with an intraperitoneal injection of 5% sodium pentobarbital (0.2 mL injection/100 g weight) and a local injection of

2% lidocaine hydrochloride to the eyelids and surrounding tissue, before operation for removal of eyeballs from animal bodies.

5.2. *Intracellular labeling of retinal ganglion cells (alpha cells) by microelectrodes*

For intracellular labeling of retinal ganglion cells (alpha cells), the eye was removed from animals and hemisected. The retina was isolated from the pigment epithelium and the vitreous humor was removed. The isolated retina was placed on filter membrane paper (Millipore cat. No. AAWG01300; Bedford, MA, USA) in photoreceptor cell-side down, using slight suction to make them adhere. The tissue was transferred to Ames' medium (which is buffered with 1.9 g/L sodium bicarbonate and continuously bubbled with a gas mixture of 95% O_2 and 5% CO_2), placed in a superfusion chamber with retinal ganglion cells-side up, and maintained at 30–35°C. The perfusion chamber was mounted on the stage of a fixed-stage upright light microscope (E-600FN type, Nikon, Tokyo, Japan), equipped with a microincubator (PMSI; Harvard, Holliston, MA, USA). The tissue was perfused at 1 mL/min with filtered Ames' medium, equilibrated with 95% O_2-5% CO_2. The tissue was viewed through a 40X/0.80NA, water immersion, long-working-distance objective (Nikon). Cell bodies of α-GCs were identified by the size (more than 20 μm in diameter) and their characteristic nuclei (Hidaka *et al.*, 2004) under Nomarski differential interference illumination.

Intracellular Neurobiotin labeling was obtained from retinal ganglion cells (alpha cells) in retinal whole-mounted preparations using microelectrode fashion. Micropipettes were pulled from boroscilicate glass capillaries (outer diameter, 1.0 mm; inner diameter, 0.58 mm, Clark Electromedical Instruments, Pangbourne, England) with a vertical pipette puller (Model 700C, David Kopf Instruments, Tujunga, CA, USA), filled at their tips with 6% Neurobiotin (Vector Laboratories, Burlingame, CA, USA) and 3% Lucifer Yellow (Aldrich, Milwaukee, WI, USA), dissolved in 0.5M LiCl and 0.05M Tris buffer (pH 7.6), and then backfilled with 3M potassium acetate. Lucifer Yellow (LY) was used for identification of the success of intracellular impalement into neurons by micropipettes. Final DC resistances of these microelectrodes ranged from 350 to 450 Mohm. Individual retinal ganglion cells (alpha cells) was impaled with an electrode connected with a high-impedance amplifier (MEZ-8301, Nihon Kohdenn, Tokyo, Japan). Neurobiotin and LY were then injected into the cell, by passing polarized currents of +1 nA, duration of 500 ms, at 1 Hz for 2–10 min (Hidaka *et al.*, 2004).

Electrophysiological characterization of retinal ganglion cells was performed by single whole-cell recordings using a patch pipette filled with an intracellular solution (see below) involving 0.5% Neurobiotin and 0.1% LY. The Neurobiotin-injected retinas were fixed in fixative containing 4% paraformaldehyde and 0.15 M NaCl in 0.1 M phosphate buffer saline (PBS), pH 7.4, for 2 h at room temperature. Following fluorescent microscopical confirmation of LY labeling of individual injected cells

February 6, 2017 6:17:07pm WSPC/179-JIN 1650031 ISSN: 0219-6352 2nd Reading

under a blue excitation (Nikon), the localization of Neurobiotin was visualized by incubation with a solution of either avidin–biotin–HRP complex (ABC; Elite kit; Vector Laboratories) in PBS (pH 7.5) or horseradish peroxidase streptavidin (Vector Laboratories) in PBS (pH 7.8), and followed by the reaction with diaminobenzidine (DAB; Dozin, Tokyo, Japan). Tracer coupling and dendrodendritic connections between retinal ganglion cells (alpha cells) were microscopically examined and photographed in color positive films (Fujichrome PROVIA 400F). Images were taken into a PC-type computer using Adobe Photoshop application program, equipped with a 35 mm film scanner (LS-1000; Nikon). Neurobiotin-labeled specimens were also utilized for electron microscopic analysis (see below).

5.3. *Dual whole-cell patch-clamp recordings of electrical synapses*

The electrical coupling between alpha-type retinal ganglion cells (alpha cells) described below was measured from pairs of cells in retinal flat-mounted preparations. Electrophysiological characterization of electrical synapses between retinal ganglion cells (alpha cells) was performed by dual whole-cell recordings using patch pipettes filled with an intracellular solution (see below) involving 0.5% Neurobiotin and 0.1% LY. For whole-cell recordings of these cells, LY was used for identification of success of intracellular recordings into neurons by patch pipettes. Recordings were made from these cells *in situ* to identify retinal ganglion cells (alpha cells) by the characteristic morphology of their somata and dendritic extension (Peichl *et al.*, 1987; Peichl, 1989; Tauchi *et al.*, 1992; Hidaka *et al.*, 2002, 2004). The somata of retinal ganglion cells (alpha cells) were exposed by either mechanical disruption of the retina's surface using fine forceps operation or enzymatic removal of the Muller glia endfeet and the inner limiting membrane by treating the retina with papain. A modification of the enzymatic processing of the rabbit retina, developed by Velte and Masland (1999), was used for exposition of retinal ganglion cell (alpha cells) somata in the albino rat retinas. The tissue was incubated in the following activated enzyme solution: 20 U/mL papain (Worthington biochemical, Lakewood, NJ, USA; cat. No. LS003126), 1 mM L-cysteine, 0.5 mM EDTA in Earl's balanced salt solution (BSS) at 37°C for 10–30 min. To stop the enzymatic digestion, 10 mg/mL Ovomucoid and 10 mg/mL bovine serum albumin (BSA) were applied for 5 min in Earl's BSS (all Sigma). After washing, the retina was treated with 0.2 Kunitz U/mL DNase I (Worthington biochemical, cat. No. LS002172) for 10 min at 37°C. In the experiments, the extracellular solution for incubation of the retinas contained (in mM): 125 NaCl, 2.5 KCl, 2.5 $CaCl_2$, 1 $MgCl_2$, 25 $NaHCO_3$, 25 glucose (305–315 mosmol/kg), and continuously bubbled with 95% O_2-5% CO_2 at 30–35°C. Chemicals were added to the external solution. The concentrations of the chemicals were as follows (in μM): 30 3-(2-carboxypiperazin-4-yl)-propanephosphonic acid (CPP), 10 6-cyanol-7-nitroquinoxaline-2,3-dione (CNQX), 10 bicuculine, 1 strychnine, 2500 $CoCl_2$ (all Sigma), 1 tetrodotoxin (TTX; Sankyo, Tokyo, Japan).

February 6, 2017 6:17:07pm WSPC/179-JIN 1650031 ISSN: 0219-6352 2nd Reading

Simultaneous dual whole-cell recordings were performed in ruptured-patch mode (Sakmann & Neher, 1995; Hidaka & Ishida, 1998; Hidaka *et al.*, 2004; Hidaka, 2012), using dual Axopatch 200B amplifiers (Axon Instruments, Foster city, CA, USA). Pipettes were pulled with the P-97 model pipette puller (Sutter Instruments, Novato, CA, USA) from borosilicate glass capillaries (outer diameter, 1.5 mm; inner diameter, 0.86 mm, Sutter Instruments) to tip resistances of 3.5–5 Mohm. Pipette (intracellular) solution consisted of (in mM): 117 K-gluconate, 13 KCl, 3.4 NaCl, 1 $CaCl_2$, 2 $MgCl_2$, 10 1,2-bis(2-aminophenoxy)ethane-N,N,N',N'-tetraacetic acid (BAPTA), 10 HEPES, 5 Mg-ATP, 0.8 Na_2GTP. LY was added (1–5 μg/μL) to the internal solution (0.1–0.5%), and the pH of this solution was adjusted to 7.3 with potassium hydroxide solution (total K^+ concentration was 140 mM). Osmolarity was adjusted to 285–295 mosmol/kg with sucrose. Closely located large cell bodies of more than 20 μm in diameter were first approached by dual electrodes under the bright field illumination. We targeted two larger cell bodies of about 100–200 μm apart, because they could probably be selected for retinal ganglion cells (alpha cells) of the same morphological type (Peichl, 1989; Peichl *et al.*, 1987; Tauchi *et al.*, 1992). Cell bodies of alpha retinal ganglion cells were identified by the size (more than 20 μm in diameter) and their characteristic nuclei (Tauchi *et al.*, 1992) under Nomarski differential interference illumination. Then, these cells were sequentially patched using LY-filled pipettes. When individual dendrites of these cells were once filled with the dye under fluorescent observation, the presence of dendritic contacts could be identified. Alpha retinal ganglion cells of the same type expanding their dendrites in the same sublayer of the IPL: i.e., the same physiological type (Famiglietti *et al.*, 1997; Dowling, 1987) were connected with each other at their dendrites (Hidaka *et al.*, 2004). After we established the whole-cell mode, cells were generally held at a membrane potential of −60 mV. The holding potentials were corrected for liquid junction potentials.

Depolarizing and hyperpolarizing current pulses were applied to one of the potentially coupled retinal ganglion cells (alpha cells). Voltage responses recorded in current-clamp mode from the other cell indicated electrical coupling between these neurons. The coupling coefficient between two cells was determined as the ratio of the voltage response in cell 2 divided by the voltage response in cell 1 under steady-state conditions. The fast current-clamp feedback circuitry of the Axopatch 200B was used in all current-clamp recordings. Current protocols and off-line analysis were performed with the pCLAMP 9 system (Axon Instruments). The voltage monitor output of the patch-clamp amplifier was analog-filtered with a Bessel filter that built-in to the Axopatch 200B (corner frequency = 1 kHz) and digitally sampled at twice the filter frequency (or faster). Series resistance typically measured less than 15 Mohm (range of values measured at the beginning of current measurements from individual cells: 7–14 Mohm). Cells with series resistance above 17 Mohm were excluded from analysis.

5.4. *Examination of the effects by intracellular cyclic nucleotides on electrical synapses*

For control condition and perfusion with dopamine or 8-bromo-cyclic AMP (8-br-cAMP) (Sigma), the tips of patch electrodes were filled with LY and either biocytin or Neurobiotin dissolved in an inner solution. To examine the effects of intracellular cyclic nucleotides on the opening of gap junctions between retinal ganglion cells (alpha cells), the tips of patch electrodes were involved with cyclic nucleotide (cAMP or cGMP) (Sigma), together with LY and the biotinylated tracer. When multiple substances involved at the tips of patch electrodes were, at the same concentration, ejected by passing the polarized currents in the time duration, the currents can equilibrate both influx of the biotinylated tracer and cAMP from the glass electrode into the cell in the electrophoresis.

To examine the effects of intracellular cyclic nucleotides on the electrical synapses between retinal ganglion cells (alpha cells), the patch electrodes were involved with 5 mM cAMP or cGMP (Sigma). The concentration of cyclic nucleotides effective to electrical synapses between retinal ganglion cells (alpha cells) was experimentally determined. When the internal solution involves cyclic nucleotides, the pH of the solution was also adjusted to 7.5 with potassium hydroxide solution (total K^+ concentration, 145 mM). Data are presented as mean ± SEM. Statistical significance was evaluated by Student's *t*-test.

5.5. *Immunocytochemical analysis of connexin expression*

Seven female rats were used for immunocytochemical studies under deep anesthesia with pentobarbital. Aldehyde-based fixative was utilized in examination of connexin36 (Cx36) localization in retinal tissue. The specificity of anti-Cx36 antibody was examined in our previous papers (Hidaka *et al.*, 2002, 2004). For paraformaldehyde-based fixation, animals were perfused quickly through the ascending aorta with a fixative containing 4% paraformaldehyde in 0.1 M PBS (pH 7.4). Fixed tissue was washed in PBS and immersed in PBS containing 20% sucrose for cryoprotection. The tissue was embedded in O.C.T. compound (Miles, Elkhart, IN), sectioned (10–20 μm) on a cryostat (Leica, Nussloch, Germany) at -20°C, and mounted on gelatin-coated slides. Cryosections were dried at -20°C or -80°C. The sections were incubated in a blocking solution of 3% normal goat serum to block nonspecific binding, and then incubated with the anti-Cx36 antibody (diluted 1:1000 with PBS). Control cryosections were incubated in rabbit preimmune serum. The specimens were then incubated in goat anti-rabbit IgG (H + L), conjugated with Alexa Fluor 546 (absorption 556 nm/max emission 575 nm, Molecular Probes, Eugene, OR). The Cx36-labeled specimens were examined under an epifluorescence microscope with a green excitation (Nikon, Tokyo, Japan) for the Alexa Fluor 546 fluorescent labeling. Fluorescent images were also taken on a confocal microscope (see next). For Cx36 localization probed by Alexa Fluor 546, fluorescent images were taken on a confocal laser-scanning microscope (Carl Zeiss LSM710, Germany),

using the 543 nm line of a helium-neon laser under the 560 nm long pass filter. For double labeling immunofluorescence of Cx36 on identified neurons, images were obtained on the LSM710, using the Multi-Scan function with a combination of the 543 nm laser under the 560 nm cut filter for Cx36, and the 458 nm line of an argon laser under a band pass filter of 475–545 nm for LY labeling of retinal ganglion cells or the 488 nm laser under a band pass filter of 500–530 nm for LY labeling visualized by anti- LY antibody (Sigma) probed by Alexa Fluor 488. Digital images acquired from the confocal microscope were processed in Abobe Photoshop (Adobe System, Inc.; San Jose, CA) to adjust brightness and color contrast of the multichannel signals.

5.6. *Examination of the effects by connexin antibodies on electrical synapses between retinal ganglion cells (alpha cells)*

Gap junctions between alpha-type retinal ganglion cells (alpha cells) are labeled with the anti-Cx36 antibody (see Results). These results suggest that binding to gap junctions between alpha cells by the anti-Cx36 antibody will affect physiological properties of those electrical synapses. To examine the effects of the anti-Cx36 antibody on the electrical synapses, patch electrodes were involved with some concentration of the antibody. The concentration of the anti-Cx36 antibody was measured for proteins of antibody IgG with the absorption of proteins dissolved in PBS, according to Kurosawa *et al.* (2009)(see below). In brief, the absorption of proteins was measured with an absorption spectrophotometer (BIOSPEC-1600, Shimazu, Tokyo, Japan) using OD 280 nm. Concentration of the anti-Cx36 antibody in PBS was calculated from an equation of the absorption multiplied with the absorption coefficient of IgG proteins (1.4 mg/mL). In some experiments, the tips of patch pipettes were included with several doses of anti-Cx36 antibody (see Results). The concentration of the antibody effective to electrical synapses between retinal ganglion cells (alpha cells) was experimentally determined. In other experiments, the tips of patch pipettes were involved with cocktail of 5 mM cAMP and doses of anti-Cx36 antibody (see Results). As negative-control antibody to anti-Cx36 antibody, anti-connexin (Cx43) antibody (Chemicon International, Billerica, MA) was utilized in this study. When the internal solution involves the antibody, the pH of the solution was also adjusted to 7.5 with potassium hydroxide solution (total K^+ concentration, 145 mM).

5.7. *Electron microscopic analysis*

According to methods previously described for three-dimensional analysis of dendrodendritic connections between Neurobiotin-labeled alpha cells by high-voltage electron microscopy (Hidaka *et al.*, 1986, 1989, 1993, 2004, 2005, 2008; Shimoda *et al.*, 1992), the DAB visualization was performed by the heavy metal intensification of horseradish peroxidase (HRP) reaction in the presence of 0.1 M $(NH_4)_2Ni(SO_4)_2$ and 0.1 M $CoCl_2$, dissolved in 0.1 M Tris buffer, pH 7.8 (see Adams, 1981). The

February 6, 2017 6:17:07pm WSPC/179-JIN 1650031 ISSN: 0219-6352 2nd Reading

reaction products were further processed by the photochromic intensification with 0.02% nitro blue tetrazolium (Sigma), dissolved in 0.1 M Tris buffer, pH 8.2, under green excitation of fluorescent microscopy (see Vaney, 1992). Prior to electron microscopical analysis of dendrodendritic connections between the cells, the specimens were examined light-microscopically.

For ultrastructural examination of connections between alpha cells, tissues were postfixed in 1% OsO_4 in PBS, dehydrated in a series of ethanol-water mixtures, and embedded in a mixture of Epoxy resins involving Glycidether 100 (Serva, Heidelberg, Germany). To enhance electron density of the specimens for high-voltage electron microscopical analysis of thick sections, en bloc stainings were made in three steps of 3% $K_2Cr_2O_7$ in D.W., 2% uranyl acetate in 70% ethanol and 20% phosphotungstic acid in the absolute ethanol. Serial tangential sections (5 μm in thickness) of the cells to be studied were made (see Hidaka *et al.*, 1986, 2004, 2005), and the material was examined in a HITACHI H-1250M high-voltage electron microscope at 1000 kV (National Institute for Physiological Sciences, Okazaki, Japan). For analysis of junctional structures between the interconnected dendrites of retinal ganglion cells, serial ultrathin sections from the specimens were studied in a JEM 1010, JEOL 1200EX or HITACHI H-7000, H-7650 conventional electron microscope at 75 kV or 80 kV fitted with a goniometer stage.

For immuno-electron microscopic analysis of gap junctions involving Cx36, isolated retinas were mounted on Millipore membrane filters in the photoreceptor-side down by slight suction, and then fixed in a fixative containing 4% paraformaldehyde in 0.1 M PBS (pH 7.4). Following PBS wash, retinas were cut into slices in 1 mm width for electron microscopical analysis. After cryoprotection in PBS containing 20% sucrose and the freeze-thaw procedure in liquid nitrogen, specimens were incubated with the primary antibody (see above). After PBS washes, the specimens were incubated in secondary antibodies of either goat anti-rabbit IgG ($F(ab')_2$) conjugated with HRP (Histofine Simple Stain MAX PO-R, Nichirei, Tokyo, Japan) or biotin-conjugated goat anti-rabbit IgG (Medical Biological Laboratory: MBL, Nagoya, Japan). The latter preparation was followed by incubation with the ABC solution (Vector Lab.). The immunocytochemical localization was then visualized by the DAB reaction.

Acknowledgments

This work was supported by JSPS KAKENHI Grant Number JP15K08193 to S.H. Our studies were performed in the 21st-Century COE Program to Fujita Health University (Directors: Drs. Yoshizo Asano and Yoshikazu Kurosawa) from the Japanese Ministry of Education, Culture, Sports, Science and Technology. This work was also in part supported by the Science Research Promotion Fund from the Promotion and Mutual Aid Corporation for Private Schools of Japan (Number 231016), and by Grants-in-Aid for Scientific Research from the Japanese Ministry of Education, Culture, Sports, Science and Technology to S.H. (Number 03857020 and 04857016 and 10680754). I am grateful to Dr. Roman R. Poznanski for reading the

first draft of this manuscript, and providing helpful suggestions for improvement. My high-voltage electron microscopical studies were performed in the co-operative program of National Institute for Physiological Sciences (Okazaki, Japan) with numbers of 2012-HVEM504, 2013-HVEM506, 2014-HVEM502 and 2015-HVEM503. I greatly appreciate Drs. Kazuyoshi Murata, Katsumi Kato, Tatsuo Arii and Noboru Yamaguchi for excellent maintenance of the HITACHI H-1250M electron microscope and valuable advice pertaining to ultrastructural studies. I thank Drs. Gen Niini, Hideki Imada, Toshiaki Kato, Yang Lu and Yoko Hashimoto for technical advice pertaining to ultrastructural and histochemical experiments, and Chieko Nishikawa, Masayo Kamiya, Michiyo Maehara, Keiichi Iizuka, Daisuke Ishihara, Junko Ikoma and Mayu Watanabe for technical assistance.

REFERENCES

Adams, J.C. (1981) Heavy metal intensification of DAB-based HRP reaction product. *J. Histochem. Cytochem.*, **29**, 775.

Barlow, H.B., Fitzhugh, R. & Kuffler, S.W. (1957) Change of organization in the receptive fields of the cat's retina during dark adaptation. *J. Physiol.* **137**, 338–354.

Bennett, M.V.L., Barrio, L.C., Bargiello, T.A., Spay, D.C., Hertzberg, E., Saez, J.C. (1991) Gap junctions: New tools, new answers, new questions. *Neuron*, **6**, 305–317.

Bloomfield, S.A. & Völgyi, B. (2004) Function and plasticity of homologous coupling between AII amacrine cells. *Vision Res.*, **44**, 3297–3306.

Bloomfield, S.A. & Völgyi, B. (2009) The diverse functional roles and regulation of neuronal gap junctions in the retina. *Nat. Rev. Neurosci.*, **10**, 495–506.

Bruzzone, R., White, T.W. & Paul, D.L. (1996) Connections with connexins: The molecular basis of direct intercellular signaling. *Eur. J. Biochem.*, **238**, 1–27.

Dacheux, R.F. & Raviola, E. (1986) The rod pathway in the rabbit retina: A depolarizing bipolar and amacrine cell. *J. Neurosci.*, **6**, 331–345.

Dermietzel, R., Kremer, M., Paputsoglu, G., Stang, A., Skerrett, I.M., Gomes, D., Srinivas, M., Janssen-Bienhold, U., Weiler, R., Nicholson, B.J., Bruzzone, R. & Spray, D.C. (2000) Molecular and functional diversity of neural connexins in the retina. *J. Neurosci.*, **20**, 8331–8343.

Dowling, J.E. (1987) *The Retina: An Approachable Part of the Brain.* Massachusetts: Harvard University Press.

Famiglietti, E.V., Kaneko, A. & Tachibana, M. (1977) Neuronal architecture of ON and OFF pathways to ganglion cells in carp retina. *Science*, **198**, 1267–1269.

Goodenough, D.A., Goliger, J.A. & Paul, D.L. (1996) Connexins, connexons, and intercellular communication. *Annu. Rev. Biochem.*, **65**, 75–502.

Hampson, E.C.G.M., Vaney, D. I. & Weiler, R. (1992) Dopaminergic modulation of gap junction permeability between amacrine cells in mammalian retina. *J. Neurosci.*, **12**(12), 4911–4922.

Hidaka, S. (2012) Suppression of electrical synapses between retinal amacrine cells of goldfish by intracellular cyclic-AMP. *Brain Res.*, **1449**, 1–14.

Hidaka, S., Akahori, Y. & Kurosawa, Y. (2004) Dendrodendritic electrical synapses between mammalian retinal ganglion cells. *J. Neurosci.*, **24**(46), 10553–10567.

Hidaka, S., Christensen, B.N. & Naka, K. (1986) The synaptic ultrastructure in the outer plexiform layer of the catfish retina: A three-dimensional study with HVEM and conventional EM of Golgi-impregnated bipolar and horizontal cells. *J. Comput. Neurol.*, **247**, 181–199.

Hidaka, S. & Ishida, A.T. (1998) Voltage-gated Na^+ current availability after step- and spike-shaped conditioning depolarizations of retinal ganglion cells. *Pflügers Arch.*, **436**, 497–508.

Hidaka, S., Kato, T. & Miyachi, E. (2002) Expression of gap junction connexin36 in adult rat retinal ganglion cells. *J. Integr. Neurosci.*, **1**(1), 3–22.

Hidaka, S., Kato, T. & Hashimoto, Y. (2005) Structural and functional properties of homologous electrical synapses between retinal amacrine cells. *J. Integr. Neurosci.*, **4**(3), 313–340.

Hidaka, S., Shingai, R., Dowling, J.E. & Naka, K. (1989) Junctions form between catfish horizontal cells in culture. *Brain Res.*, **498**, 53–63.

Hidaka, S., Maehara, M., Umino, O., Lu, Y. & Hashimoto, Y. (1993) Lateral gap junction connections between retinal amacrine cells summating sustained responses. *Neuroreport*, **5**, 29–32.

Janssen-Bienhold, U., Dermietzel, R. & Weiler, R. (1998) Distribution of connexin43 immunoreactivity in the retinas of different vertebrates. *J. Comput. Neurol.* **396**(3), 310–321.

Kolb, H. & Nelsen, R. (1983) Rod pathways in the retina of the cat. *Vision Res.*, **23**, 301–312.

Kothmann, W.W., Massey, S.C. & O'Brien, J. (2009) Dopamine-stimulated dephosphorylation of connexin 36 mediates AII amacrine cell uncoupling. *J. Neurosci.*, **29**(47), 14903–14911.

Kurosawa, G., Akahori, Y. & Kurosawa, G. (2009) Comprehensive screening for antigens overexpressed on carcinomas via isolation of human mAbs that may be therapeutic. *Proc. Natl. Acad. Sci. USA*, **105**(20), 7287–7292.

Mastronarde, D.N. (1983) Correlated firma of cat retinal aanalion cells. II. Responses of X- and Y-cells to single quanta1 events. *J. Neurophysiol.*, **49**, 325–349.

Mastronarde, D.N. (1989) Correlated firing of cat retinal ganglion cells. *Trends Neurosci.*, **12**, 75–80.

Meister, M., Lagnado, L. & Baylor, D.A. (1995) Concerted signaling by retinal ganglion cells. *Science* **270**, 1207–1210.

Miyazaki, S., Yuzaki, M., Nakada, K., Shirakawa, H., Nakanishi, S., Nakade, S. & Mikoshiba, K. (1992) Block of Ca^{2+} wave and Ca^{2+} oscillation by antibody to the inositol 1,4,5-trisphosphate receptor in fertilized hamster eggs. *Science*, **257**(5067), 251–255.

Muller, J.F. & Dacheux, R.F. (1997) Alpha ganglion cells of the rabbit retina lose antagonistic surround responses under dark adaptation. *Vis Neurosci*, **14**, 395–401.

Naka, K. & Christensen, B.N. (1981) Direct electrical connections between transient amacrine cells in the catfish retina. *Science*, **214**, 462–464.

Nelson, R. (1982) AI1 amacrine cells quicken time course of rod signals in the cat retina. *J. Neurophysiol.*, **47**, 928–947.

Peichl, L. (1989) Alpha and delta ganglion cells in the rat retina. *J. Comput. Neurol.*, **286**, 120–139.

Peichl, L., Ott, H. & Boycott, B.B. (1987) Alpha ganglion cells in mammalian retinae. *Proc. R. Soc. Lond. B. Biol. Sci.*, **231**, 169–197.

February 6, 2017 6:17:08pm WSPC/179-JIN 1650031 ISSN: 0219-6352 2nd Reading

Peichl L. & Wässle, H. (1983) The structural correlate of the receptive field centre of ganglion cells in the cat retina. *J. Physiol. (Lond.)*, **341**, 309–324.

Penn, A.A., Wong, R.O.L. & Shatz, C.L. (1994) Neuronal coupling in the developing mammalian retina. *J. Neurosci.*, **14**, 3805–3815.

Sakmann, B. & Neher, E. (1995) *Single-Channel Recording*. 2nd edn. N.Y: Plenum Press.

Shimoda, Y., Hidaka, S., Maehara, M., Lu, Y. & Hashimoto, Y. (1992). Hyperpolarizing interplexiform cell of the dace retina identified physiologically and morphologically. *Vis. Neurosci.*, **8**(3), 193–199.

Söhl, G., Maxeiner, S. & Willecke, K. (2005) Expression and functions of neuronal gap junctions. *Nat. Rev. Neurosci.*, **6**(3), 191–200.

Tauchi, M., Morigiwa, K. & Fukuda, Y. (1992) Morphological comparisons between outer and inner ramifying alpha cells of the albino rat retina. *Exp. Brain Res.*, **88**, 67–77.

Umino, O., Maehara, M., Hidaka, S., Kita, K. & Hashimoto, Y. (1994) The network properties of bipolar-bipolar coupling in the retina of teleost fishes. *Vis. Neurosci.*, **11**, 533–548.

Vaney, D.I. (1991) Many diverse types of retinal neurons show tracer coupling when injected with biocytin or Neurobiotin. *Neurosci. Lett.*, **125**, 187–190.

Vaney, D.I. (1992). Photochromic intensification of diaminobenzidine reaction product in the presence of tetrazolium salts: Applications for intracellular labelling and immunohistochemistry. *J. Neurosci. Methods*, **44**, 217–223.

Vaney, D.I. (1994) Patterns of neuronal coupling in the retina, In: N. N.Osborne & G. J. Chader, eds. *Progress in Retinal Eye Research*, Vol. 13, Oxford: Pergamon Press, pp. 301–355.

Velte, T.J. & Masland, R.H. (1999) Action potentials in the dendrites of retinal ganglion cells. *J Neurophysiol*, **81**, 1412–1417.

Völgyi, B., Kovács-Öller, T., Atlasz, T., Wilhelm, M. & Gábriel, R. (2013) Gap junctional coupling in the vertebrate retina: Variations on one theme? *Prog. Retinal Eye Res.*, **34**, 1–18.

White, T.W. & Paul, D.L. (1999) Genetic diseases and gene knockouts reveal diverse connexin functions. *Annu. Rev. Physiol.*, **61**, 283–310.